



NONLINEAR SEISMIC RESPONSE OF IRREGULARLY MASONRY-INFILLED R.C. FRAMED BUILDINGS RETROFITTED WITH HYSTERETIC DAMPED BRACES

F. Mazza⁽¹⁾, M. Mazza⁽²⁾, A. Vulcano⁽³⁾

⁽¹⁾ Researcher, Dipartimento di Ingegneria Civile, Università della Calabria, Rende (Cosenza), Italy, fabio.mazza@unical.it

⁽²⁾ Research fellow, Dipartimento di Ingegneria Civile, Università della Calabria, Rende (Cosenza), Italy, mirko.mazza@unical.it

⁽³⁾ Full professor, Dipartimento di Ingegneria Civile, Università della Calabria, Rende (Cosenza), Italy, alfonso.vulcano@unical.it

Abstract

An irregular in-elevation distribution of the infill walls in a reinforced concrete (r.c.) framed building can produce significant variations in stiffness, strength and mass distribution leading to severe seismic damage. To mitigate these effects and retrofit the structure, hysteretic damped braces (HYDBs) can be suitably inserted in the framed structure. The retrofitting criteria are aimed to obtain a damped braced structure globally regular with regard to stiffness and strength. In detail, the stiffness distribution of HYDBs is evaluated consistently with a constant value of the drift ratio of the damped braced frame along the building height; moreover, the strength distribution of the HYDBs is assumed so that their activation tends to occur at every storey simultaneously, before reaching the shear resistance of the infilled framed structure. For proportioning the HYDBs, a Displacement-Based Design (DBD) procedure, in which the design starts from a target deformation of an equivalent elastic linear system, is adopted in the present work. To check the effectiveness and reliability of the DBD procedure, a numerical investigation is carried out with reference to a six-storey r.c. framed building, which, originally designed according to an old Italian seismic code (1996) for a medium-risk zone, has to be retrofitted by inserting of HYDBs to attain performance levels imposed by the current Italian code (NTC 2008) in a high-risk zone. It is supposed that the irregularity is consequent to a change in use of the first two floors, from residential to office, substituting the masonry infills of the first three storeys with glass windows. Nonlinear dynamic analyses of the unbraced, irregularly infilled and damped braced infilled frames are carried out by a step-by-step procedure, considering sets of artificially generated and real ground motions, whose response spectra match those adopted by NTC 2008 for different performance levels. To this end, r.c. frame members are idealized by a two-component model, assuming a bilinear moment-curvature law and considering the effect of the axial load on the ultimate bending moment of the columns. The response of an HYDB is idealized by a bilinear law, preventing buckling. Finally, masonry infills are represented as equivalent diagonal struts reacting only in compression according to an elastic-brittle law. Even though more refined analytical models can be used to simulate the hysteretic response of r.c. members and infill walls, the design procedure prove to be effective in the mitigation of the effects of the in-elevation irregular distribution of the infill walls.

Keywords: Irregularly infilled r.c. framed buildings; Seismic retrofitting; Hysteretic damped braces; Displacement-Based Design; Nonlinear dynamic analysis.



1. Introduction

Irregularities in elevation due to soft-storeys or unsymmetrical layout of infill walls can produce significant variations in stiffness, strength and mass distribution of reinforced concrete (r.c.) framed buildings, leading to severe seismic damage. To mitigate these effects and retrofit the structure, damped steel braces can be suitably inserted in the framed structure. Currently a wide variety of energy dissipating devices is available (e.g., see Soong and Dargush [1]). Current seismic codes allow for the use of these devices (e.g. European code 2003, EC8 [2]); Italian code, NTC08 [3]) but few codes provide simplified design criteria (e.g. FEMA 35 [4]).

A Displacement-Based Design (DBD) procedure (Mazza et al. [5]), in which the design starts from a target deformation of an equivalent elastic linear system with effective properties (see Priestley et al. [6]) is adopted in the present work for the seismic retrofitting of a six-storey r.c. framed structure exhibiting an in-elevation irregularity of the masonry infills. The retrofitting criteria are aimed to obtain a damped braced structure, using hysteretic damped braces (HYDBs), globally regular with regard to stiffness and strength. To check the effectiveness and reliability of the design procedure, a numerical investigation is carried out supposing that the r.c. framed building, originally designed according to a previous Italian code (DM96 [7]) for a medium-risk zone, has to be retrofitted by inserting of HYDBs to comply with NTC08 in a high-risk zone. Nonlinear dynamic analyses of unbraced (UF), irregularly infilled (IF) and damped braced infilled (DBIF) frames are carried out by a step-by-step procedure, considering sets of artificially generated and real ground motions, whose response spectra match those adopted by NTC08 for different performance levels.

2. Displacement-based design of hysteretic damped braces

A DBD procedure proposed by Mazza and Vulcano [8, 9] for proportioning the HYDBs in order to attain a designated performance level of an existing r.c. regular framed structure for a specific level of seismic intensity, was extended to framed buildings with irregular distribution of masonry infills in-plan (Mazza [10]) or in-elevation (Mazza et al. [5]). The main steps of this procedure are summarized below.

1. Pushover analysis of the unbraced (bare) frame and definition of an equivalent single degree of freedom (ESDOF) system to evaluate the equivalent viscous damping due to hysteresis

Nonlinear static (pushover) analysis of a given unbraced frame under constant gravity loads and monotonically increasing horizontal loads, is carried out to obtain the base shear-top displacement ($V^{(F)}$ - d) curve (Fig. 1a). For this purpose, the lowest capacity curve is selected assuming the most common lateral-load profiles: e.g. proportional to the floor masses (m_1, m_2, \dots, m_n) or referring to the inverted-triangular shape or first-mode shape. The selected $V^{(F)}$ - d curve can be idealized as bilinear and the original frame can be represented by an ESDOF system (Fajfar [11]) characterized by a bilinear curve (V^* - d^*), with a yield displacement $d_y^{(F)}$ and a stiffness hardening ratio r_F , derived from the idealized $V^{(F)}$ - d curve (Fig. 1b). Once the displacement (d_p) and the corresponding base shear ($V_p^{(F)}$) are settled, for a given performance level, the ductility (μ_F) and the equivalent (secant) stiffness ($K_e^{(F)}$) can be evaluated for the frame:

$$\mu_F = d_p / d_y^{(F)} \quad (1)$$

$$K_e^{(F)} = V_p^{(F)} / d_p \quad (2)$$

The equivalent viscous damping due to hysteresis of the framed structure, $\xi_F^{(h)}$, can be calculated as:

$$\xi_F^{(h)} (\%) = \kappa 63.7 \frac{(\mu_F - 1)(1 - r_F)}{[\mu_F + \mu_F r_F (\mu_F - 1)]} \quad (3)$$

where μ_F and r_F have been defined above. As the inelastic displacements may be underestimated due to the overestimation of the equivalent damping, a reduction factor κ is considered in Eq. (3), e.g. derived through nonlinear dynamic analyses (Mazza and Vulcano [12]). In particular, according to ATC 40 [13], κ can be assumed equal to 1/3 in the case of poor structural behaviour.



2. Equivalent viscous damping due to hysteresis of the damped braces

If the constitutive law of the equivalent damped brace is idealized as bilinear (Fig. 1c), the viscous damping, $\xi_{DB} = \xi_{DB}(\mu_{DB}, r_{DB})$, being μ_{DB} and r_{DB} , respectively, the ductility demand and the stiffness hardening ratio, can be evaluated by an expression analogous to Eq. (3). Also ξ_{DB} , for the same reasons emphasized above for $\xi_F^{(h)}$, may be suitably reduced. The ductility demand of the equivalent damped brace, μ_{DB} , can be evaluated as

$$\mu_{DB} = \left[1 + (\mu_D - 1)(1 + r_D K_D^*) \right] / (1 + K_D^*) \quad (4)$$

μ_D being the damper ductility, whose value should be compatible with the deformation capacity of the damper itself, r_D the stiffness hardening ratio of the damper and $K_D^* (= K_D / K_B)$ the stiffness ratio reasonably assumed as rather less than 1. The stiffness of a damped brace (K_{DB}) can be expressed as depending on the brace stiffness (K_B) and the elastic stiffness of the damper (K_D):

$$K_{DB} = 1 / (1/K_B + 1/K_D) \quad (5)$$

The stiffness hardening ratio of the damped brace, r_{DB} , can be expressed as

$$r_{DB} = \frac{(1/K_B + 1/K_D)}{[1/K_B + 1/(r_D K_D)]} = r_D \frac{(1 + K_D^*)}{(1 + r_D K_D^*)} \quad (6)$$

where K_B , K_D , r_D and K_D^* have been defined above.

3. Equivalent viscous damping of the frame with damped braces

Assuming a suitable value of the elastic viscous damping for the framed structure (e.g. $\xi_V = 5\%$), the equivalent viscous damping of the in-parallel system comprised of framed structure (F) and damped braces (DBs) is

$$\xi_e (\%) = \xi_V + \frac{[\xi_F^{(h)} V_p^{(F)} + \xi_{DB} V_p^{(DB)}]}{[V_p^{(F)} + V_p^{(DB)}]} \quad (7)$$

where $\xi_F^{(h)}$ and ξ_{DB} have been calculated in steps 1 and 2, respectively, $V_p^{(F)}$ has been defined above and $V_p^{(DB)}$ represents the base-shear contribution due to the damped braces of the damped braced frame (DBF) at the performance point. Then, with reference to the displacement spectrum for ξ_e , the effective period (T_e) of the DBF can be evaluated as that corresponding to the performance displacement d_p .

4. Effective stiffness of the equivalent damped brace for retrofitting in-elevation regular and irregular framed structures

Once the mass of the ESDOF system ($m_e = \sum m_i \phi_i$) is calculated, the effective stiffness of DBF (K_e) and the effective stiffness required by the damped braces ($K_e^{(DB)}$) can be evaluated as

$$K_e = 4\pi^2 m_e / T_e^2, \quad K_e^{(DB)} = K_e - K_e^{(F)} \quad (8a,b)$$

5a. Effective strength properties of the equivalent damped brace for retrofitting the in-elevation regular framed structure

Because the base shear-displacement curve representing the response of the damped braces of the actual structure ($V^{(DB)}$ -d) has been idealized as bilinear, the base-shear contributions of the damped braces at the performance and yielding points ($V_p^{(DB)}$ and $V_y^{(DB)}$, respectively) can be calculated:

$$V_p^{(DB)} = K_e^{(DB)} d_p \quad (9)$$

$$V_y^{(DB)} = V_p^{(DB)} / [1 + r_{DB} (\mu_{DB} - 1)] \quad (10)$$

Note that the equivalent viscous damping expressed by Eq. (7) depends on the base-shear $V_p^{(DB)}$, which is initially unknown. As a consequence, an iterative procedure is needed for the solution of Eqs. (7)-(10).



5b. Strength properties of the hysteretic damped braces for retrofitting the in-elevation irregular framed structure

On the other hand, the strength properties of the equivalent damped brace evaluated in the step 5a have been not considered for the in-elevation irregular structure, because the strength distribution of the HYDBs is assumed so that their activation occurs at every storey simultaneously, at the same time or before the attainment of the yield shear of the infilled framed structure. More specifically, the strength distribution of the HYDBs is such that their yielding shear force ($V_{yi}^{*(DB)}$) is reached, at each storey, before (or simultaneously) the attainment of the ultimate values of frame ($V_{ui}^{(F)}$) and infill ($V_{ui}^{(I)}$) shear forces:

$$V_{yi}^{*(DB)} = \min(V_{ui}^{(F)}; V_{ui}^{(I)}), \quad i=1, \dots, n \quad (11)$$

To force a simultaneous yielding of the HYDBs, the distribution law of the yielding shear force in the HYDBs ($V_{yi}^{(DB)}$) is modified be similar to that of the (elastic) shear force induced by the lateral loads ($V_{di}^{(DB)}$), e.g. assuming an inverted-triangular shape, as will be specified in the step 6b (see Fig. 1d):

$$V_{yi}^{(DB)} = V_{yi}^{*(DB)} \frac{\alpha_{V, \min}^{(DB)}}{\alpha_{Vi}^{(DB)}}, \quad i=1, \dots, n \quad (12)$$

where

$$\alpha_{Vi}^{(DB)} = \frac{V_{yi}^{*(DB)}}{V_{di}^{(DB)}}, \quad \alpha_{V, \min}^{(DB)} = \min[\alpha_{Vi}^{(DB)}] \quad (13a,b)$$

In this way, the shear ratio of the HYDBs, defined as the ratio between their actual shear ($V_{yi}^{(DB)}$) and the shear required by the analysis ($V_{di}^{(DB)}$), is constant along the building height.

6a. Design of the hysteretic damped braces of the damped braced frame for retrofitting the in-elevation regular framed structure

For an in-elevation regular infilled framed structure, according to the proportional stiffness criterion ([8, 9]), it can be reasonably assumed that a mode shape (e.g. the first-mode shape: $\{\phi_1, \dots, \phi_n\}^T$) of the primary frame remains practically the same even after the insertion of damped braces. Then, the distribution of the lateral loads carried by the damped braces at the yielding point ($d_y^{(DB)}$) can be assumed proportional to the stiffness distribution. These design criteria are preferable in the case of the retrofitting of in-elevation regular structure, because the stress distribution in the frame members remains practically unchanged. Once the shear at a generic storey is calculated as (see $F_{yi}^{(DB)}$ forces in Fig. 1d)

$$V_{yi}^{(DB)} = \sum_{j=i}^n F_{yj}^{(DB)} = \sum_{j=i}^n \frac{m_j \phi_j}{\sum_{k=i}^n m_k \phi_k} V_y^{(DB)} \quad (14)$$

the quantities needed for designing the damped brace at that storey can be determined. In particular, for a single diagonal HYDB (Fig. 1d), the yield-load and the elastic (diagonal) stiffness can be respectively calculated as

$$N_{yi} = V_{yi}^{(DB)} / (2 \cos \alpha_i) \quad (15)$$

$$K_i^{(DB)} = \frac{1}{2(\phi_i - \phi_{i-1})d_y^{(DB)}} \frac{1}{\cos \alpha_i^2} V_{yi}^{(DB)} \quad (16)$$

6b. Design of the hysteretic damped braces of the damped braced frame for retrofitting the in-elevation irregular framed structure

Alternatively to step 6a, the criteria followed for an in-elevation irregular infilled framed structure are aimed to obtain a damped braced structure globally regular in stiffness. For this purpose, assuming an inverted-triangular (linear) shape (ϕ_{lin}), the corresponding shear forces ($V_{lin}^{(DB)}$) of the damped braced frame are calculated as

$$V_{lin}^{(DBF)} = \left\{ \sum_{j=1}^n m_j \phi_{lin,j}, \dots, \sum_{j=1}^n m_j \phi_{lin,j}, \dots, m_n \phi_{lin,n} \right\}^T \quad (17)$$

Then, the lateral stiffness of the damped braced frame ($K_i^{(DBF)}$), consistently with a constant value of the drift ratio (=interstorey drift/height storey= Δ_i/h_i) (Fig. 1d), can be evaluated assuming

$$\frac{K_i^{(DBF)}}{K_1^{(DBF)}} = \frac{V_{lin,i}^{(DBF)} h_1}{V_{lin,1}^{(DBF)} h_i}, \quad i=2, \dots, n \quad (18)$$

while the lateral stiffness of the damped braces ($K_i^{(DB)}$) can be obtained from the lateral stiffness of the existing frame ($K_i^{(F)}$) for Δ_i/h_i constant:

$$K_i^{(DB)} = K_i^{(DBF)} - K_i^{(F)}, \quad i=1, \dots, n \quad (19)$$

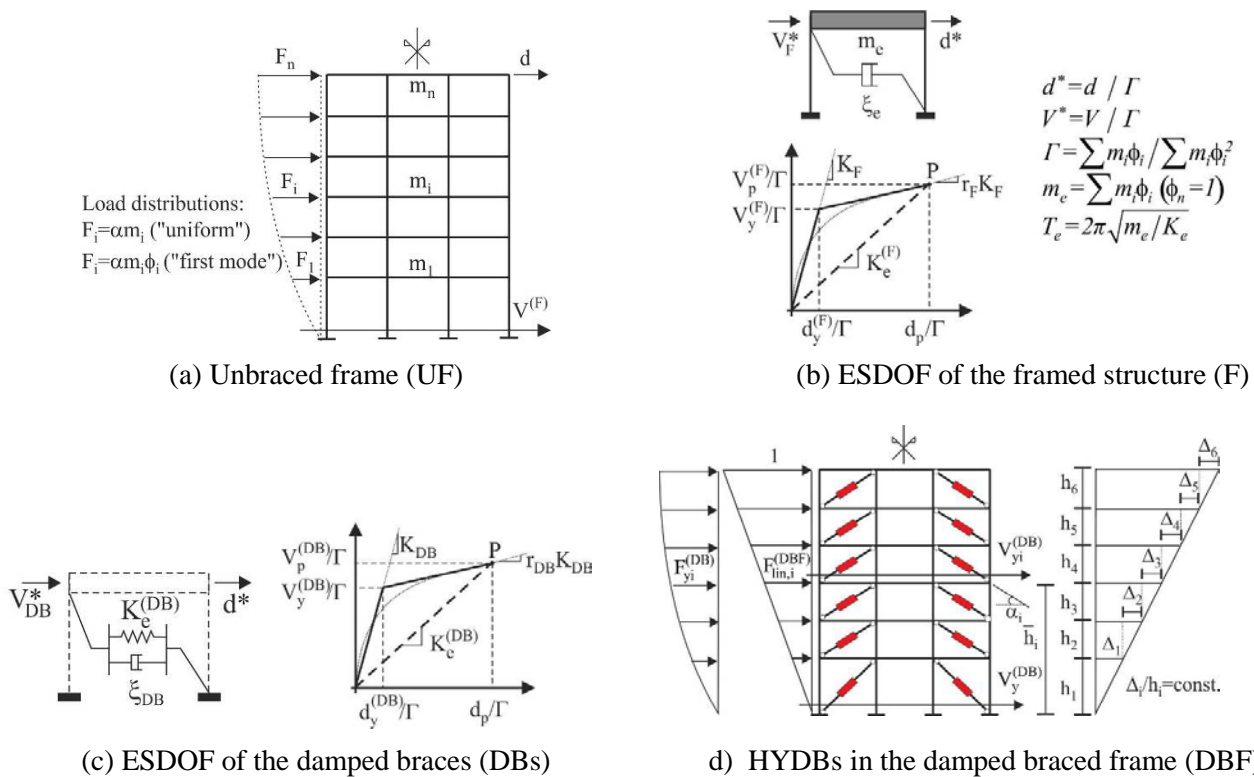


Fig. 1 – Main assumptions for designing the hysteretic damped braces (HYDBs)

Finally, the sum of all the stiffness of the damped braces at every storey can be assumed to be equal to the effective stiffness evaluated by Eq. (8b) of step 4:

$$\left(\sum_{i=1}^n K_i^{(DB)} \right)_{Irregular} = K_e^{(DB)} \quad (20)$$

As can be observed, the assumption of a same value of $K_e^{(DB)}$ for the in-elevation regular and irregular buildings makes comparable these structural solutions. In particular, Eqs. (18)-(20) represent a linear system in the $2n$ unknown stiffness parameters of the HYDBs (i.e. $K_i^{(DB)}$, $i=1, \dots, n$) and damped braced frame (i.e. $K_i^{(DBF)}$, $i=1, \dots, n$), with assigned values of the unbraced frame stiffness (i.e. $K_i^{(F)}$, $i=1, \dots, n$), corresponding to a constant drift ratio along the height of the structure, and effective stiffness of the equivalent damped brace (i.e. $K_e^{(DB)}$).

3. Layout and design of the test structure

A six-storey building with a r.c. framed structure, whose symmetric plan is shown in Fig. 2a, is considered as primary test structure, where masonry infill walls are regularly distributed along the perimeter (Fig. 2a) and in elevation (Fig. 2b). To simulate a vertical irregularity, it is supposed that, due to a change in use of the first two floors of the building, from residential to office, masonry infill walls of the lower three storeys are substituted with glass windows (Fig. 2c) and an increased live load is considered on the first and second floors.

A simulated design of the original framed building is carried out in accordance with a previous Italian seismic code (DM96), for a medium-risk seismic region (seismic coefficient: $C=0.07$) and a typical subsoil class (main coefficients: $R=\epsilon=\beta=1$). The gravity loads for the r.c. framed structure are represented by a dead load of 4.2 kN/m^2 on the top floor and 5.0 kN/m^2 on the other floors, and a live load of 2.0 kN/m^2 on all the floors; an average weight of about 2.7 kN/m^2 is considered for the masonry infill walls. More precisely, each masonry infill is supposed as made with two layers of perforated bricks, with a thickness of 12 cm (exterior) and 8 cm (interior). Concrete cylindrical compressive strength of 25 N/mm^2 and steel reinforcement with yield strength of 375 N/mm^2 are considered. The design is carried out to comply with the ultimate limit states. Detailing for local ductility is also imposed to satisfy minimum conditions for the longitudinal bars of the r.c. frame members.

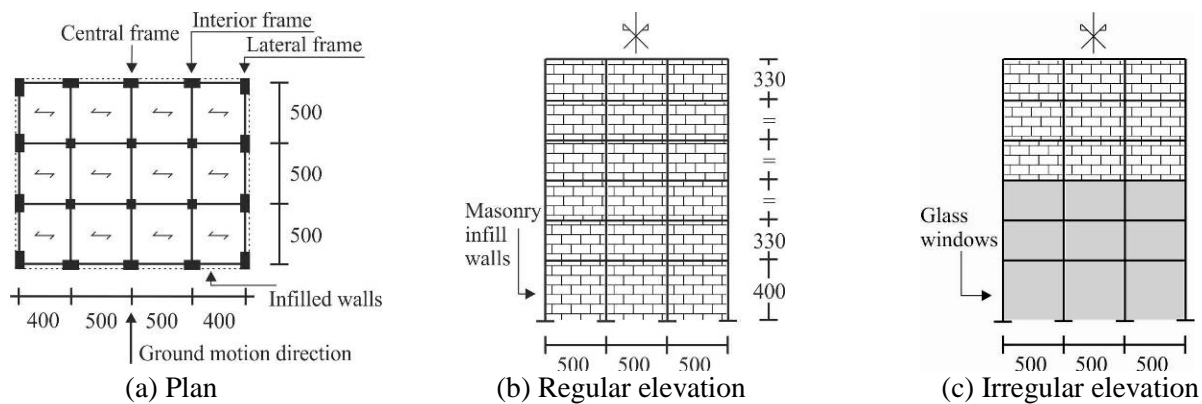
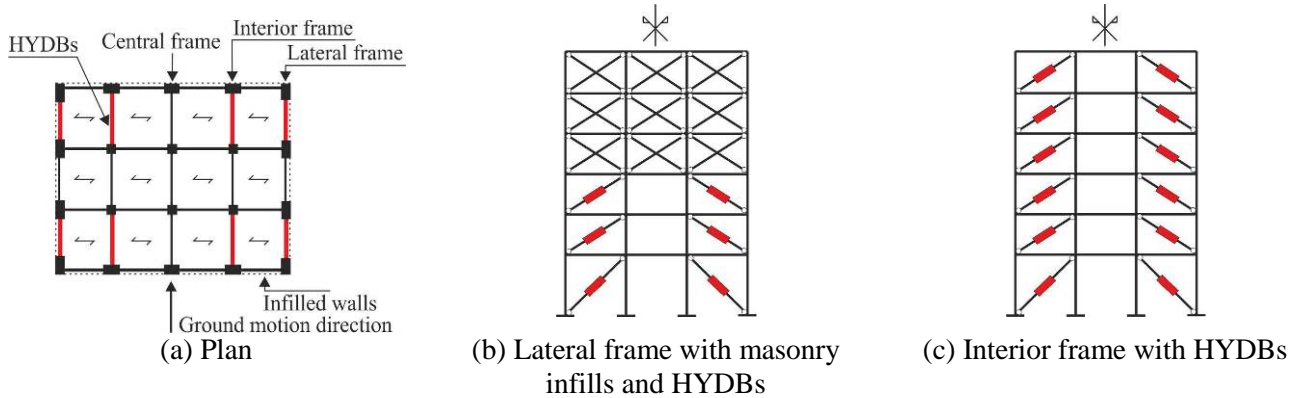
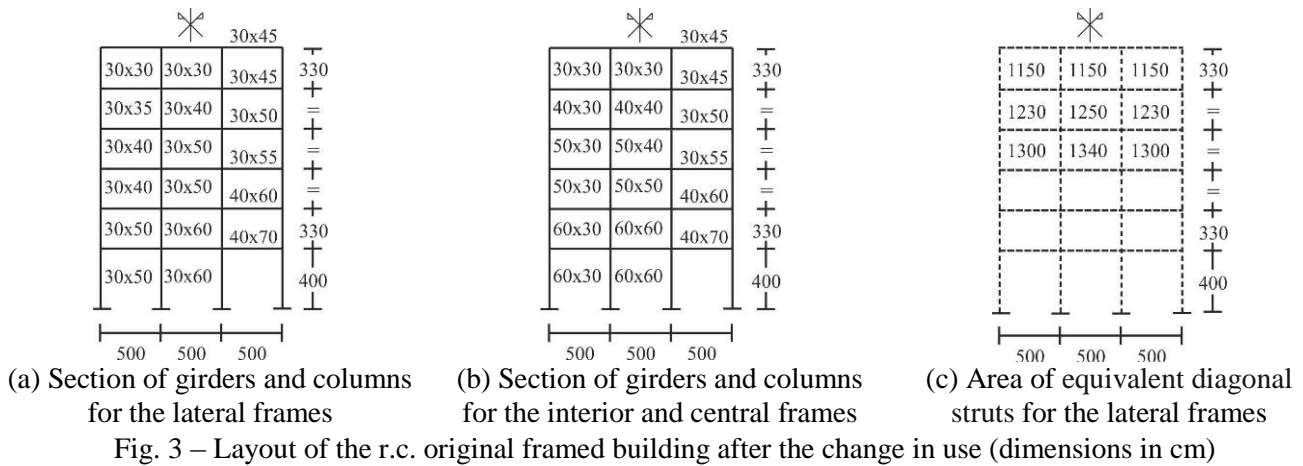


Fig. 2 – Test structure (dimension in cm)

After the change in use, glass windows with an average weight of 0.21 kN/m^2 and a live load of 3.0 kN/m^2 have been considered on the first two floors. The stiffness and strength contributions of the glass windows are neglected, but those of the masonry infill walls in the upper three storeys are considered evaluating the area of an equivalent diagonal strut as suggested by Mainstone [14]).

The geometric dimensions and size of the sections of the original frames are shown in Fig. 3a (i.e. lateral frames) and Fig. 3b (i.e. interior and central frames), while the area of the equivalent diagonal struts representing masonry infill walls on the upper three floors of the lateral frames are shown in Fig. 3c. Ultimate values of the curvature ductility, not reported for brevity, are evaluated for the r.c. frame members in accordance with the provisions of EC8 for the assessment of existing buildings.

To upgrade the irregularly infilled frame (IF) from a medium- to a high-risk seismic region, diagonal steel braces with hysteretic dampers (HYDs) are inserted at each storey. For simplicity, in Fig. 4a only HYDBs in the frames along the considered ground motion direction are shown. Both design procedures for in-elevation regular (i.e. DBIF_R) and irregular (i.e. DBIF_IR) infilled framed structures are applied to the same r.c. structure. The DBIF_R and DBIF_IR structures are characterized by the same HYDBs at the first three storeys of the lateral frames (Fig. 4b) but different HYDBs at all storeys of the interior frames (Fig. 4c). More specifically, HYDBs with stiffness and strength properties equal to those of the masonry infills existing before the change in use are placed in the exterior bays of the lateral frames (at the first three storeys), while a pair of equivalent diagonal struts represent the masonry walls placed at the upper three storeys (Fig. 4b). Moreover, HYDBs are placed in the exterior bays of the interior frames, at all storeys (Fig. 4c), in accordance with the design criteria discussed above for the DBIF_R (i.e. steps 5a and 6a of the previous section) and DBIF_IR (i.e. steps 5b and 6b of the previous section) structures.



The main dynamic properties of the original (i.e. UF and IF) and retrofitted structures (i.e. DBIF_R and DBIF_IR) are reported in Table 1: i.e. fundamental vibration period (T_1) and ratio of the corresponding effective mass ($m_{E,1}$) to the total mass (m_t), with reference to the ground motion direction. As noted in ref. [5], the value of T_1 for the IF structure is lower than that for the UF structure, because a reduced mass is supposed at the first three storeys, where masonry infill walls are substituted with glass windows (whereas the mass of the infills at all storeys is considered in UF structure), and an increased lateral stiffness is considered at the upper three storeys due to the contribution of the masonry infills (nowhere considered in UF structure).

The HYDBs in Fig. 4c are designed considering seismic loads provided by NTC08 for a high-risk seismic region and subsoil class B. In Table 2, the following data are reported for damage (SLD), life-safety (SLV) and collapse (SLC) limit states, i.e.: peak ground acceleration on rock, a_g ; site amplification factor, $S=S_S \cdot S_T$, S_S and S_T being factors accounting for subsoil and topographic characteristics, respectively; peak ground acceleration $PGA(=a_g \times S)$. More precisely, the ratios of a_g and PGA to the gravity acceleration (g) are reported.

To avoid brittle behaviour of the r.c. structure, a design value of the frame ductility $\mu_F=1.0 \times \gamma_{SLV} = 1.5$, assuming e.g. a safety factor $\gamma_{SLV}=1.5$, is considered at the life-safety limit state (SLV). Further details regarding dynamic properties, lateral stiffness and shear force along the height of the original (i.e. UF and IF) and retrofitted (i.e. DBIF_R and DBIF_IR) structures can be found in ref. [5]. In particular, a brace rigid enough that its deformability can be neglected is assumed for the DBIF_R and DBIF_IR structures (then, according to Eq. (5), $K_{DB}=K_D$ can be assumed). Also different values of the lateral stiffness of the frame have been obtained, because a different shape for lateral forces has been assumed for DBIF_R and DBIF_IR structures: i.e. first vibration mode and inverted-triangular (linear) shape, respectively.



Table 1– Dynamic properties of the original (UF and IF) and retrofitted (DBIF_R and DBIF_IR) structures

Properties	UF	IF	DBIF_R	DBIF_IR
T_1 (s)	0.746	0.602	0.203	0.203
$m_{E,1} / m_t$	0.75	0.89	0.70	0.70

Table 2 – Seismic design parameters (NTC08)

Limit states	a_g / g (*)	S	PGA/g (*)
SLD	0.094	1.20	0.11
SLV	0.270	1.13	0.31
SLC	0.351	1.05	0.37

(*) g = gravity acceleration

4. Numerical results

To check the effectiveness and reliability of the DBD design procedure illustrated above, a numerical investigation is carried out considering also the contribution of the infill walls. Then, the nonlinear dynamic responses of the unbraced (UF), infilled (IF) and damped braced infilled (DBIF) frames, when subjected to sets of artificial and real ground motions, are compared. To this end, sets of three artificial motions, generated by the computer code SIMQKE (Gasparini and Vanmarcke [15]), and sets of seven real motions, selected by the computer code REXEL (Iervolino et al. [16]), are considered with reference to the serviceability (i.e. damage, SLD) and ultimate (i.e. life-safety, SLV, and collapse, SLC) limit states imposed by NTC08. More specifically, the response spectra of artificial and real accelerograms match, on average, NTC08 spectra for a subsoil class B (see Table 2) in the range of vibration periods 0.05s-2s, which also contains the lower and upper limits of the vibration period prescribed by EC8 (i.e. $T_{min}=0.2T_1$ and $T_{max}=2T_1$, in the case $T_1 \leq 1s$)

Because of the structural symmetry and assuming the floor slabs to be infinitely rigid on their own plane, the entire structure (see Figs. 2 and 4) is idealized by an equivalent plane frame (pseudo-three-dimensional model) along the considered horizontal ground motion direction. Nonlinear dynamic analyses are carried out by a step-by-step procedure (Mazza F and Mazza M [17]), assuming elastic-perfectly laws to simulate the response of the r.c. frame members and HYDBs; in particular for the columns, the effect of the axial load on the ultimate moment is taken into account. As mentioned above, each infill wall is represented as a pair of equivalent diagonal struts connecting the frame joints (see Fig. 4b) and reacting in compression only (that is, one at a time under horizontal loading). More precisely, the response of a diagonal strut is simulated by an elastic linear force-displacement law, assuming that an infill wall collapses when the ultimate strength is reached (brittle failure). The damping matrix of the structure is assumed as a linear combination of the mass and stiffness matrices, assuming a viscous damping ratio of 5% associated with the first and third vibration periods. All the following results are obtained as an average of those separately obtained for the sets of artificial or real motions corresponding to a limit state.

Firstly, results obtained under the SLD, SLV and SLC sets of artificial ground motions are shown in Figs. 5-7, considering the original (i.e. UF and IF) and retrofitted (i.e. DBIF_R and DBIF_IR) structures. In particular, the ductility demand to the r.c. frame members has been calculated in terms of curvature, with reference to the two loading directions, assuming as yielding curvature for the columns the one corresponding to the axial force due to the gravity loads. It is worth mentioning that the analyses were interrupted, for all the examined cases, once the ultimate value imposed on the curvature ductility demand of the r.c. frame members was reached, but this happened at different instants in time ($t_{max}^{(k)}$). For this reason, the analyses were repeated assuming, for all structures, the minimum final instant of simulation (t_{min} , i.e. minimum of the $t_{max}^{(k)}$ values).

As can be observed, comparable ductility demands to r.c. members have been obtained for the UF and IF structures, at all limit states. The insertion of HYDBs is effective in reducing the ductility demand of girders (Figs. 5a and 6a), with similar curves for the DBIF_R and DBIF_IR structures. However, as shown in Fig. 7a, columns of the second and third storeys exhibit a maximum ductility demand in the DBIF_R structure slightly



greater than that obtained in the UF and IF structures. This kind of behaviour can be interpreted by observing that the DBIF_R structure is characterized by values of the axial load in the columns higher than those in the original structures. Further results, omitted for the sake of brevity, have confirmed that the balanced compressive load is exceeded in some columns of the DBIF_R structure, at the lower three storeys, under SLV and SLC motions. Finally, for all the structures the maximum axial load is resulted much less than the ultimate compressive axial load and no tensile axial loads have been found.

To check the effectiveness of the design procedure for proportioning the HYDBs so that an in-elevation regular framed structure is obtained and the hysteretic energy dissipated by the devices be as large as possible, the maximum values of the drift ratio at the SLD (Fig. 5b) and SLV (Fig. 6b), and ductility demand of the HYDBs at the SLC (Fig. 7b) are plotted at each storey. As shown, the irregular distribution law of the drift ratio for the IF structure become almost uniform with reduced values in the DBIF_IR structure at the SLD (in the quasi-elastic range), and in the DBIF_R structure at the SLV. As can be observed, the distribution of the HYDB ductility demand (at the SLC) is almost uniform in all storeys and rather less than the design value (i.e. $\mu_D=10$) for the DBIF_R structure, unlike in the case of the DBIF_IR structure where there is a considerable variability, with a mean ductility demand of about 13.2.

To further clarify the effectiveness of the HYDBs for reducing the damage of the r.c. frame members, a time ratio α_t , defined as the ratio between the time corresponding to reaching the ultimate curvature of some critical section of the frame members (t_{max}) and the total duration of the artificial motions (i.e. $t_{tot}=12s$), is plotted in Fig. 8. Note that a value of α_t equal to 1 is obtained at the SLD (results are omitted for brevity), for the original and retrofitted structures, and at the SLV, with the only exception being the UF structure (Fig. 8a). On the other hand, the total duration of the artificial motions at the SLC is attained only for the DBIF_R and DBIF_IR structures (Fig. 8b), while the analysis was terminated earlier for the UF and IF structures.

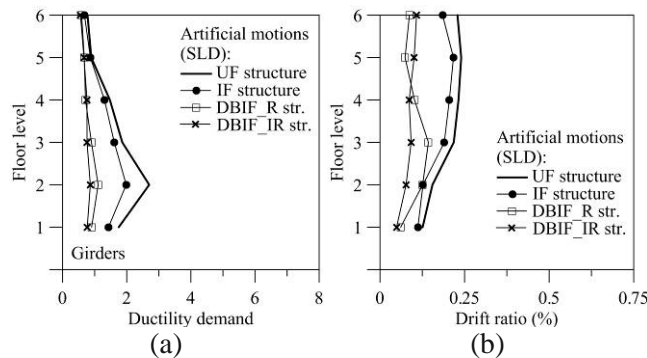


Fig. 5 – Maximum ductility demand to girders (a) and drift ratio (b) under SLD artificial motions (simulation duration: $t_{tot}=12$ s)

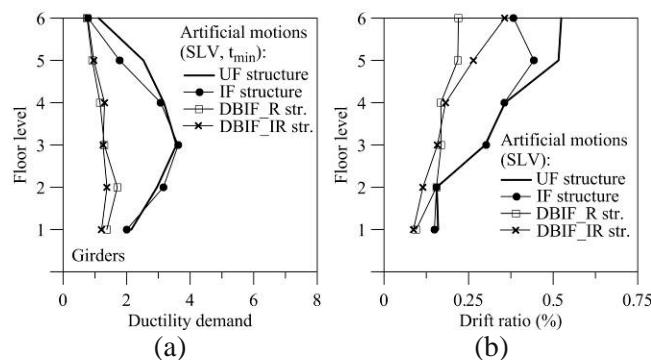


Fig. 6 – Maximum ductility demand to girders (a) and drift ratio (b) under SLV artificial motions, assuming the minimum final instant of simulation for all structures ($t_{min}=2.29s$)

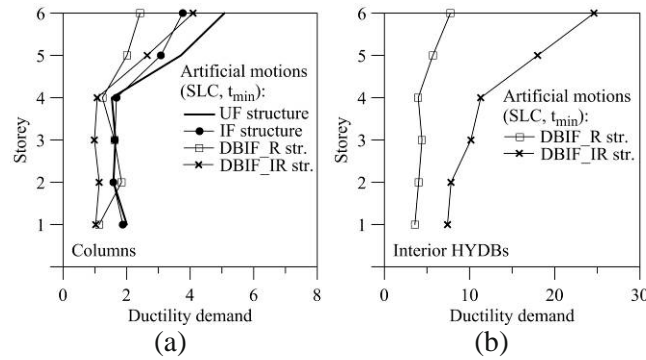


Fig. 7– Maximum ductility demand to columns (a) and HYDBs (b) under SLC artificial motions, assuming the minimum final instant of simulation for all structures ($t_{min}=2.28s$)

Ductility curves analogous to those illustrated above are shown in Fig. 9 with reference to the SLV artificial motions, assuming the maximum final instant of simulation ($t_{max}^{(k)}$) for each structure. It should be noted that the response of the UF structure, characterized by a limited duration of the analysis (i.e. $\alpha_t=0.19$) due to the attainment of the ultimate ductility demand in some r.c. frame members, appears generally better than that observed for the IF structure, but the total duration of motion (i.e. $\alpha_t=1$) is attained for the latter structure. Moreover, damage control of the girders appears more effective with the DBIF_IR structure rather than the DBIF_R one, especially at the lower storeys, differently from that observed at the minimum final instant of simulation for all structures (see Fig. 6a).

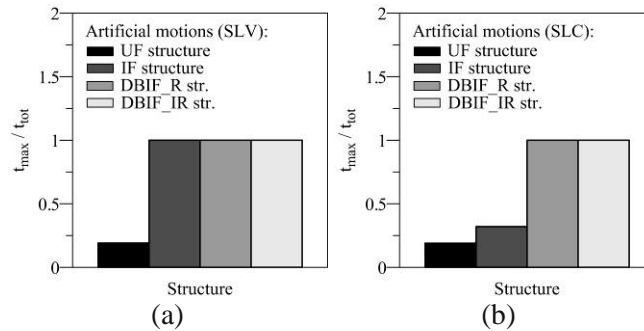


Fig. 8 – Time ratio ($\alpha_t=t_{max}/t_{tot}$) for all structures under SLD, SLV and SLC artificial motions

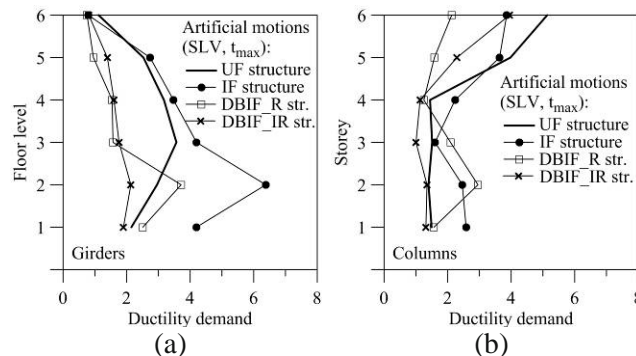


Fig. 9 – Maximum ductility demand to r.c. frame members under SLV artificial motions, assuming the maximum final instant of simulation ($t_{max}^{(k)}$) for each structure

To check the reliability of the design procedure, maximum top displacement (Fig. 10a) and maximum storey displacement (Fig. 10b) of original (i.e. UF and IF) and retrofitted (i.e. DBIF_R and DBIF_IR) structures are reported. Specifically, SLV artificial motions are considered, assuming the maximum final instant of simulation of each structure. As can be observed, a conservative evaluation of about 8% of the design



displacement (d_p) has been obtained at the top storey of the DBIF_R structure; whereas, d_p in the DBIF_IR structure has been exceeded of about 19%. Finally, maximum storey displacement of the DBIF_R and DBIF_IR structures were always less than the design value, except only at the top storey of DBIF_IR structure (Fig. 10b).

Finally, ductility demands on girders (Fig. 11a) and columns (Fig. 11b) of a lateral frame are plotted under SLV real motions, assuming t_{min} for all structures. Apart from some differences, the results are similar to those, omitted for brevity, were obtained for interior and central frames. Conclusions analogous to those illustrated above for artificial motions (see Figs. 6a and 7a) can be drawn.

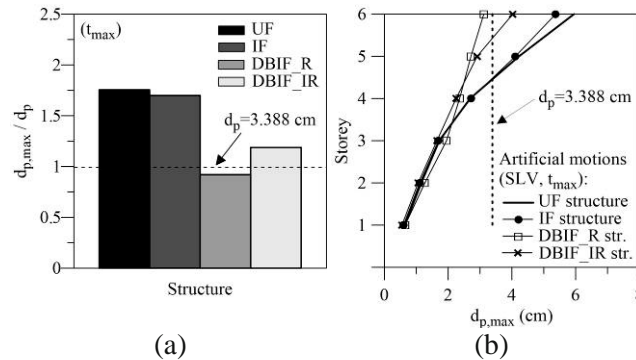


Fig. 10 – Maximum top displacement (a) and maximum storey displacement (b) of original (i.e. UF and IF) and retrofitted (i.e. DBIF_R and DBIF_IR) structures under SLV artificial ground motions

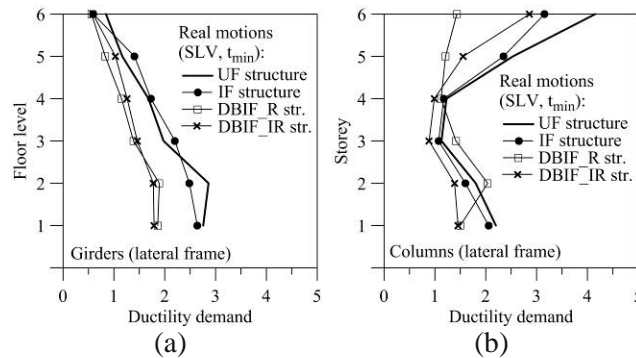


Fig. 11 – Maximum ductility demand on girders and columns of a lateral frame under SLV real motions, assuming the minimum final instant of simulation (t_{min}) for all structures

5. Conclusions

A DBD procedure of HYDBs previously proposed for seismic retrofitting of regular framed structures has been extended to framed structures with an in-elevation infill irregularity, supposing that, due to a change in use from residential to office of a six-storey r.c. residential building, masonry infills are replaced by glass windows in the first three storeys. To check effectiveness and reliability of the design procedure, the nonlinear seismic responses of unbraced (UF), irregularly infilled (IF) and damped braced infilled (DBIF_R and DBIF_IR) frames have been studied.

The response of the IF structure was comparable with that of the UF frame, assuming the minimum final instant of simulation (t_{min}) for both structures. However, the UF structure generally behaved better than the IF structure, with reference to the maximum final instant (t_{max}), but a total duration of the simulation equal to or less than that of the IF structure was obtained. Comparable reduction damage of r.c. members was found with the DBIF_R and DBIF_IR structures and referring to t_{min} , but the DBIF_IR structure proved to be more effective than the DBIF_R one considering t_{max} . The DBIF_IR structure was retrofitted for the life-safety limit state but also worked well for the damage and collapse ones. A damper ductility demand almost uniform, rather less than



the design value, was obtained for the DBIF_R structure, while a wide variability, with a mean value greater than the design one, was observed for the DBIF_IR structure.

Further improvements in the validation of the design procedure can be obtained by a more refined modelling of the r.c. members and masonry walls, accounting for degradation of their mechanical properties.

6. Acknowledgements

The present work was financed by Re.L.U.I.S. (Italian network of university laboratories of earthquake engineering), in accordance with “Convenzione D.P.C.–Re.L.U.I.S. 2014–16, WPI, Isolation and Dissipation”.

7. References

- [1] Soong TT, Dargush GF (1997): Passive Energy Dissipation Systems in Structural Engineering. *John Wiley & Sons Ltd*, Chichester, England.
- [2] Eurocode 8 (2003): Design of structures for earthquake resistance - part 1: general rules, seismic actions and rules for buildings. *C.E.N., European Committee for Standardization*.
- [3] NTC08 (2008): Technical Regulations for the Constructions. *Italian Ministry of the Infrastructures, D.M. 14-01-2008 and Circ. 02-02-2009 n. 617/C.S.LL.PP* (in Italian).
- [4] Federal Emergency Management Agency, FEMA 356 (2000): Prestandard and commentary for the seismic rehabilitation of buildings. *American Society of Civil Engineers*, Reston, Virginia.
- [5] Mazza F, Mazza M, Vulcano A. (2015): Displacement-based seismic design of hysteretic damped braces for retrofitting in-elevation irregular r.c.framed structures. *Soil Dynamics and Earthquake Engineering*, **69**, 115-124.
- [6] Priestley MJN, Calvi GM, Kowalsky MJ (2007): Displacement-based seismic design of structures. *IUSS Press, Istituto Universitario di Studi Superiori di Pavia (Italy)*, Vol. 1, Redwood City, CA.
- [7] DM96 (1996): Technical Regulations for the Constructions. *Italian Ministry of Public Works, D.M. 16-01-1996 and C.M. 10-04-1997 N. 65/AA.GG* (in Italian).
- [8] Mazza F, Vulcano A (2008): Displacement-based seismic design procedure for framed buildings with dissipative braces part I: Theoretical formulation. *AIP Conference Proceedings*, **1020**(1), 1399-1406.
- [9] Mazza F, Vulcano A (2014): Design of hysteretic damped braces to improve the seismic performance of steel and r.c. framed structures. *Ingegneria Sismica*, **1**, 5-16.
- [10] Mazza F (2014): Displacement-based seismic design of hysteretic damped braces for retrofitting in-plan irregular r.c. framed structures. *Soil Dynamics and Earthquake Engineering*, **66**, 231-240.
- [11] Fajfar P (1999): Capacity spectrum method based on inelastic spectra. *Earthquake Engineering and Structural Dynamics*, **28**, 979-993.
- [12] Mazza F, Vulcano A (2014): Equivalent viscous damping for displacement-based seismic design of hysteretic damped braces for retrofitting framed buildings. *Bulletin of Earthquake Engineering*, **12**(6), 2797-2819.
- [13] Applied Technology Council, (1996): Seismic Evaluation and Retrofit of Concrete Buildings, *Rep. ATC 40*.
- [14] Mainstone RJ (1974): Supplementary note on the stiffness and strength of infilled frames. *Current Paper CP13/74, Building Research Establishment*, London.
- [15] Gasparini D, Vanmarcke E (1976): Simulated earthquake motions compatible with prescribed response spectra. *Massachusetts Institute of Technology, Department of Civil Engineering*, U.S.A..
- [16] Iervolino I, Maddaloni G, Cosenza E (2008): Eurocode 8 compliant record sets for seismic analysis of structures. *Journal of Earthquake Engineering*, **12**(1), 54-90.
- [17] Mazza F, Mazza M (2010): Nonlinear analysis of spatial framed structures by a lumped plasticity model based on the Haar Kàrmàn principle. *Computational Mechanics*, **45**, 647-664.